EVALUATION OF CATHODOLUMINESCENCE SPECTROSCOPY AS A TOOL IN PALAEOTEMPERATURE ESTIMATION

CERR CONTRACT REPORT TO MOBIL OIL CANADA

EVALUATION OF CATHODOLIMINESCENCE SPECTROSCOPY
AS A TOOL IN
PALAEOTEMPERATURE ESTIMATION

R.A. Mason, B.Sc., Ph.D., P.Geo.

Centre for Earth Resources Research,
Memorial University of Newfoundland,
St.John's, Newfoundland A1B 3X5

TABLE OF CONTENTS

- Summary
- Introduction
  - Previous Work on Natural Calcite
  - Purpose of Study
- Sample Selection
- Source Of Thermal Maturity Data
- Experimental Methods
- Results
  - Cathodoluminescence spectra
  - Cathodoluminescence Measurements
    - CL intensity
    - Emission wavelength
    - Emission band width
- Discussion Of Luminescence Data
- Regional Trends
- Discussion Of Regional Trends
- Conclusion
- Future Work
- References

TABLES

Table 1a. Sample numbers, descriptions & sources of thermal maturity data
Table 1b. Cathodoluminescence results
Table 1c. Thermal maturation indicators & calcite/dolomite ratio

LIST OF FIGURES

Figure 1. Sample locations
Figure 2. CAI data for the sample locations shown in Fig. 1
Figure 3. Spectrum of CL emission from calcite
Figure 4. CAI as a function of intensity ratio
Figure 5. Ro as a function of intensity ratio
Figure 6. TAI as a function of intensity ratio
Figure 7. Centroid (control) as a function of CAI
Figure 8. Centroid (heated sample) as a function of CAI
Figure 9. Change in wavelength on heating ($\Delta\lambda$) as a function of CAI
Figure 10. Change in wavelength on heating ($\Delta\lambda$) as a function of emission wavelength of control material
Figure 11. Emission band width of heated material as a function of CAI
Figure 12. Emission band width of heated material as a function of CAI
Figure 13. Change in emission bandwidth caused by heating (ΔFWHM)
Figure 14. Ro and TAI as a function of CAI
Figure 15. TAI as a function of Ro
Figure 16a. The $CaCo_3$ - $MgCo_3$ system (after Goldsmith & Heard, 1961)
Figure 16b. Detail of the calcite-dolomite solvus at low temperature
Figure 17. Geographical distribution of intensity ratio
Figure 18. Geographical distribution of the change in emission wavelength on heating
Figure 19. Geographical distribution of the change in emission band width on heating

SUMMARY

This report concerns the application of cathodoluminescence (CL) to the estimation of palaeotemperatures in limestones from the Cambro-Ordovician Platform sequence of Western Newfoundland. It is a continuation of the program briefly reported by Mason (1992) . The work is experimental in nature, involving laboratory heating (at 400°C) of rock samples and study of the CL spectra (obtained on powders) of heated material and equivalent unheated ("control") material. The approach taken is to to compare the CL results with conventional measures of thermal maturity (especially conodont alteration index, CAI) . The CL results comprise measurements of the intensity, wavelength of emission (centroid) and width of the emission band (full width at half maximum peak height, FWHM), together with three parameters which measure changes induced by heating. The three parameters are: (1) the intensity ration (I_H/I) which is the CL intensity from heated material divided by the CL intensity of the control; (2) the change in emission wavelength ($\Delta\lambda$) defined as centroid wavelength (heated) minus centroid wavelength (control); (3) the change in width of the emission band (ΔFWHM) , defined as FWHM (heated) minus FWHM (control) . The material studied contains both dolomite and calcite, with the calcite/dolomite ratio ranging up to 1:1, as estimated by X-ray diffraction.

The intensity ratio (I_H/I) ranges from 0.3 to 2.8, very similar to the values obtained on synthetic calcite (Mason, in press) , and confirming that the CL intensity of natural calcite can be modified by heating. It was anticipated that there should be a negative relationship between intensity ratio and CAI. This proved to be the case, however there is considerable scatter in this relationship. The magnitude of the scatter is such that measurement of a single intensity ration does not allow a reliable estimate of CAI to be made from the CL data. The scatter is attributed to the limitations of the CAI, to the possible effects of deformation and to complications arising from chemical exchange between calcite and dolomite.

The wavelength (centroid) of (Mn^{2+} activated) emission from natural calcite lies in the range 597 to 623 nm in both heated and control samples. The lower value is comparable with results from very pure synthetic calcite. The upper value lies outside the observed range for synthetic calcite (600 to 609 nm: Mason, in press) . The wavelength of emission from control material decreases with increasing CAI, although there is considerable scatter in the data. On heating, the wavelength of CL emission is changed by 0 to ±20 nm, and the width of the CL emission band (FWHM) changes by 0 to ±27 nm. The change in emission wavelength induced by heating ($\Delta\lambda$) shows a positive correlation with CAI, whereas the change in FWHM induced by heating (ΔFWHM) shows a negative correlation with CAI.

Regional trends in the intensity ratio, $\Delta\lambda$, and ΔFWHM parallel that defined by CAI: that is, thermal maturity increases from west (Port aux Port Peninsula) to east (Pistolet Bay - Quirpon - Englee areas) . Of the parameters derived from CL measurement, $\Delta\lambda$ and ΔFWHM offer good prospects for practical use in palaeothermometry, although measurements on a single sample cannot, at present, be considered reliable. Regional trends in the intensity ratio only become apparent when relatively large numbers of samples are available.

The presence of dolomite in the samples, and the more complex chemistry of rocks compared with synthetic calcite, is thought to lead to the greater complexity in their behaviour on heating (i.e., significant changes in wavelength and emission band width have not been observed in synthetic calcite) .

The correlation between the wavelength of CL emission and CAI in control material is discussed terms of partial compositional equilibration towards the limb of the calcite-dolomite solvus. Similarly, the relationship between $\Delta\lambda$ and CAI is explained
(qualitatively) by redistribution of Ca and Mg between calcite and dolomite during laboratory heating. However, there are quantitative problems with these explanations, which await resolution. In addition, the hypothesis does not explain the data pertaining to changes in FWHM induced by heating.

Refinements of the CL technique for estimating palaeotemperature are possible and desirable. The principal problem is to minimise the large variations in intensity ratio and lesser, though significant, variations in $\Delta\lambda$ and ΔFWHM found in rocks with (apparently) similar thermal histories. This may be accomplished by studying single crystal material and polished slabs of rock so that composition and CL parameters can be measured at the same locations on a micro-scale. It is highly desirable to calibrate the CL parameters directly against a reliable measure of temperature such as oxygen isotope thermometry or fluid inclusion temperature.

INTRODUCTION

The intensity of cathodoluminescence (CL) emission is normally interpreted as being a function of activator and quencher element concentrations (Machel et al. 1991). However, Mason (in press) has shown that synthetic calcite heated in the range 200 to 500°C exhibits different (usually increased) cathodoluminescence (CL) intensity compared with equivalent unheated material. This observation leads to the possibility that in natural calcite the CL intensity may be a function of both minor element chemistry and thermal history. If the contribution of thermal history to CL output could be separated from that of activator/quencher concentrations, then CL could be used as a means of palaeotemperature estimation. It is shown below that the response of natural material to heating is more complex than that of synthetic calcite, probably because of the effects composition and sample heterogeneity, but that useful information on thermal maturity can be derived from the CL spectra.

Previous Work on Natural Calcite

Mason (1992) studied a small suite of limestone from the Cambro-ordovician carbonate platform sequence of Western Newfoundland and compared the CL method with conventional indicators of thermal maturity.

The CL results showed that the effects of heating are not restricted to synthetic material, and that the magnitude of the response to heating differed among the samples. This suggested that the CL spectra may indeed contain some record of the thermal history.

However, the changes in intensity correlated poorly with the conventional thermal maturity measurements and, because of the small number of samples studied, did not allow firm conclusions to be drawn regarding the validity of the CL method.

Purpose of Study

The present program was designed to overcome the inadequate sampling of the earlier study (Mason, 1992) . The aims are to compare the CL results with conventional methods of estimating palaeotemperature and to demonstrate regional trends, if any, in the CL data.

SAMPLE SELECTION

Approximately twenty-five limestones were selected from the author's collection. In addition, the materials studied by Mason (1992) were re-examined. The latter samples were selected from a suite collected by Drs S.H. Williams and E.T. Burden, who kindly provided access to their thermal maturity data (vitrinite reflectance and pollen based thermal alteration index: see Williams
Burden 1992 for details). Samples were selected to consist predominantly of calcite, as indicated by visual inspection. This was to minimise complications in the CL spectra arising from emission lines interfering with that from calcite: Mn. in particular, dolodtones were avoided and, on a hand specimen scale, the material removed for CL study was selected to minimise the amount of contaminant dolomite. Nevertheless, X-ray diffraction (XRD) study of the powders used for the CL work shows that most samples contain some, and a few contain significant quantities of, dolomite. No attempt was made to separate coarsely crystalline calcite cement from micrite.

The selected samples cover, geographically, Western Newfoundland from the Part-au-Port Peninsula in the south to Quirpon in the north (Fig. 1) . They range in age from Lower Cambrian to Lower Ordovician. Samples prefixed F880- are from the author's collection, those labelled Mob- are from the Williams & Burden collection (they can be cross referenced to appendix 1 of Williams & Burden (1992) using the field designations given in Table 1a) . In addition to these ancient limestones, recent calcites from various localities were examined. Only one of these, a precipitate (labelled BP-1) collected from "Blue Ponds" near Corner Brook, had a measurable luminescence signal. Sample details are given in Table 1a.

SOURCE OF THERMAL MATURITY DATA

The approach taken is to compare the CL results with conventional monitors of thermal maturity, rather than with a technique yielding direct estimates of temperature, because the latter are unavailable.

Thermal maturity data [conodont alteration index (CAI), vitrinite reflectance (Ro%) and thermal alteration index (TAI)) are taken from Williams & Burden (1992). In the case of the samples labelled Mob-, the Ro% and TAI data were obtained (by the latter authors) on aliquots of the samples used here for CL study. The CAI data were compiled by William's & Burden from published sources. Thermal maturity data have been estimated for samples prefixed F880- by comparison with the sample location maps and appendix 1 of Williams & Burden (1992). Fortuitously, many of the F880- limestones of the present study were collected at the same localities as those sampled by the latter authors, in which case assignment of thermal maturity indicator values was straightforward. Where thermal maturity data are lacking for a given sample location, equivalent horizons at immediately adjacent localities of Williams & Burden (1992) were used make estimates (details for each sample are given in Table 1a).

The most complete (geographical) coverage of thermal maturity data is for CAI: this indicator is used as the primary monitor of thermal history in the present work. Fig. 2 shows the CAI data in relation to the sample locations. For two samples, F88018b and BP-1, there are no CAI data. Sample F88018b is a vein calcite which cuts deformed marble (F88018a) with CAI = 5. However, the relative timing of low-grade metamorphism and vein formation are unknown and the thermal history of the vein may differ from that of the country rock. Sample BP-1 is a Recent calcite precipitate collected from a small pond (near Corner Brook) which is actively precipitating very fine-grained calcite mud. The sample is assumed never to have been outside earth-surface temperature conditions.

EXPERIMENTAL METHODS

Samples were heated in the form of rock fragments crushed to approximately 1 mm on a side. The heating temperature and duration were 400±5°C and 18.8 to 336 hrs, respectively. Mason (in press) has shown that (in synthetic calcite) at this temperature the exact duration of heating is unimportant within the range used. Following heating, the sample and an equivalent unheated "control" were powdered and mounted for CL examination. Details of the sample preparation, mounting and heating procedures are given in Mason (1992).

It was noted by Mason (1992), and described more fully by Mason (in press), that CL intensity declines as the duration of
electron bombardment increases. Thus, it is advantageous to irradiate at any one time only that part of the sample from which a spectrum is being collected. This is difficult to achieve in a cold-cathode CL microscope owing to the broadness of the beam (typically 9 x 5mm in the Luminoscope used by Mason, 1992). Accordingly, in this study, luminescence spectra were collected on a modified electron microprobe operating at 15kV accelerating voltage with a beam diameter of approximately 30 to 50 μm. These conditions produce a beam current density (14 $\mu A/mm^2$) and spectral intensity comparable with those obtained by Mason (1992).

Seven to ten spectra were collected from each sample. Each was corrected for photomultiplier dark current and any spectral overlap (see below) , and then the average was calculated.

The wavelength scale of the monochromator was calibrated in the range 300 to 1000 nm using the emission from a mercury vapour lamp. The spectra used in measuring the CL intensity were collected in a restricted wavelength range (500 to 800 nm): consequently corrections for the photomultiplier response were not required.

Following CL work, the powder was mounted for X-ray diffraction (XRD) estimation of the proportion of dolomite. This was carried out by direct comparison between the intensities of the reflections from the (104) lattice planes of calcite and dolomite.

No attempt was made to calibrate these intensities or to compensate for preferred orientation in the XRD mounts and, consequently, the results are only semi-quantitative.

RESULTS

Cathodoluminescence spectra

A spectrum from 300 to 1000 nm is illustrated in Fig. 3. The prominent emission band near 600 nm wavelength is identical to those illustrated by Mason (1992, figs. 2 to 5) and is typical of activation by Mn^{2+} incorporated in the Ca site of calcite. In several samples the 600 nm emission band overlaps with the long wavelength "tail" of a broad band emission peaking in the blue part of the spectrum at approximately 400 nm (Fig. 3). This overlap was approximated and removed by fitting a straight line between 500 and 800 nm.

The origin of the "blue" emission band is unclear: it could be "background blue" emission from calcite,

thought to be caused by structural defects (Mason & Mariano, 1990; Machel et al., 1991), or it could originate from detrital or authigenic silicate grains.

One of the disadvantages of taking spectra from powdered heterogeneous samples is the possibility of contamination by unwanted phases, such as dolomite. Visual CL examination of polished thin sections, in which dolomite is readily identified, shows that it is non-luminescent in these rocks, either because the Mn^{2+} concentration is too low or the Fe content too high, or both (Machel et al., 1991). Careful examination of the CL spectra has also failed to reveal any evidence of emission from dolomite in any of the samples, even when the calcite/dolomite ratio (measured by XRD) is as low as 1 (Table 1c) . Such emission would be expected to produce a peak in the range 640 to 650 nm (Marshall, 1988; Mason, unpublished) and, if of sufficient intensity, to be partially resolved from the calcite: Mn emission band. The absence of dolomite interference in the spectra is fortunate because it simplifies considerably the interpretation of the spectra.

Cathodoluminescence Measurements

The CL intensity was obtained by integrating under the mean spectrum. The wavelength and width of the emission band were monitored using the centroid and full-width at half-maximum height (FWHM), respectively. Measurements of these parameters were made on each of the 7 to 10 spectra obtained from each sample. Standard errors in the intensity, centroid and FWHM were obtained from the variance in the respective parameters measured on each individual spectrum. Table 1b gives the results of the CL measurements, arranged in ascending order of intensity ratio (see below).

CL intensity. The logic behind the use of CL in calcite as a palaeothermometer, and the stimulus for the experimental approach is as follows. It is known from work on synthetic calcite that, upon heating, the CL intensity changes (usually increases) relative to control material. If natural calcite has been heated after formation, those physical processes responsible for the change in luminescence intensity may have been accomplished in the earth. Heating of such a calcite in the laboratory should produce, at most, only a modest change in CL intensity. Conversely, a natural calcite which has experienced only low temperatures should respond to laboratory heating with a significant increase in CL intensity.

Changes in the Mn^{2+} CL intensity consequent on heating were measured using an "intensity ratio" I_H/I, in which I_H is the intensity from the heated material, and I is the intensity from the control (Mason, 1992 and in press) . An intensity ratio >1 indicates a "low-temperature" calcite and an intensity ratio near 1 indicates a "high-temperature" calcite. Intensity ratios measured in this study range from 0.3 to 2.8 (Table 1b), with a standard error in the range ± 0.01 to 0.06, considerably better than was obtained by Mason (1992).

Fig 4 shows the CAI values (Table 1c) plotted against intensity ratio. Given that CAI increases with increasing temperature, there should be a negative relationship between the variables on this plot. Grouping the samples by CAI and taking the mean intensity ratio for each group it can be seen that the results conform to the expected pattern. However, the scatter of I_H/I within each group is as large as the difference between groups. Thus, measurement of the intensity ratio of a single specimen does not provide a reliable estimate of thermal maturity.

As noted above, the number of samples for which TAI and Ro% values are known, or could be estimated, is relatively low. Figs. 5 & 6 show, respectively, Ro% and TAI plotted as a function of intensity ratio. In both cases a negative relationship should exist between the conventional TMI and the intensity ratio. In the case of Ro% (Fig. 5), it is possible to interpret the expected trend for four of the samples but the majority form a tight cluster which is clearly separated from this apparent trend. In Fig. 6, six of the samples may define the expected negative relationship against intensity ratio. However, at least five, and possibly seven, samples seem to define a loose cluster which violates this trend. Clearly, the interpretation of these data is ambiguous. Further discussion is presented below.

Emission wavelength. The centroid of the Mn^{2+} emission band lies in the range 597 to 623 nm (standard error <1 in both control and heated calcite (Table 1b). The lower values are comparable with results obtained on synthetic calcite (Mason, in press), for which the range is 600 to 609 nm. There is no correlation between the emission wavelength of control material and the calcite/dolomite ratio estimated from XRD data. Such a correlation would indicate spectral interference by Mn^{2+} activated emission from dolomite.

The centroids obtained on control material are plotted against CAI in Fig. 7. The data define (crudely) a trend of decreasing emission wavelength with increasing CAI, although the scatter is such that measurement of the centroid of an individual sample does not allow accurate prediction of the CAI. Fig. 8 is an equivalent plot for heated material. In this case the data do not define any clear trend. Given the precision of the centroid measurements, the scatter within each CAI class may reflect real chemical or physical differences among the materials.

From the different patterns in Figs. 7 and 8 it is clear that in some, at least, of the samples the centroid position must have changed as a consequence of heating. The change is given by:

$\Delta\lambda$ = centroid (heated) - centroid (control).

The magnitude of the change ranges up to approximately 20 nm, whereas the standard error of $\Delta\lambda$ is never worse than ±1 nm. Changes in centroid position occur in both directions, i.e. in some samples the centroid position increased upon heating and in others it decreased (Fig. 9). Within each group of samples (collected by CAI) there is considerable scatter in the extent of the change in centroid. However, the direction of change is quite consistent. Thus, most samples with CAI>3 show an increase in emission wavelength on heating and those with CAI<3 generally show a decrease. However, as with intensity ratios (Fig. 7), the CAI could not be predicted with confidence from the behaviour of a single sample.

Given the relationships illustrated in Figs. 7 and 9 it is to be expected that $\Delta\lambda$ will be related to the centroid position obtained from control material. This is illustrated in Fig. 10. Samples with a control centroid near 603 nm tend to increase emission wavelength on heating, and most have CAI > 3. Samples with a control centroid near 615 tend to decrease emission wavelength. on heating, they are also mostly samples with CAI < 3.

Emission band width. The width of the emission band, as expressed by the FWHM, varies from 71 to 93 nm for control material and 55 to 93 nm for heated material (but only one value lies outside the range 69 to 93 nm, see Table 1b) . The standard error of the measurements is dependent on the intensity of emission, but is typically ±1.5 nm. The FWHM of control material is independent of CAI (Fig. 11) but for heated material, there is a poorly defined negative relationship between FWHM and CAI (Fig. 12). This implies that, upon heating, the Mn^{2+} emission band changes in width. This change was monitored by defining

ΔFWHM = FWHM (heated) - FWHM (control).

The magnitude of ΔFWHM ranges between 0 and 27 nm (Table 1b), however, all but one sample lie in the range 0 to 12 nm. The standard error is typically ±2 nm, with a maximum of ±5 nm. Both increases and decreases in emission band width were observed. Fig. 13 shows that ΔFWHM is related systematically to the CAI. Samples from rocks with CAI <3 tend to get broader on heating whereas those from rocks with CAI = 5 generally get narrower. Both types of behaviour are observed for samples with CAI = 3.5.

DISCUSSION OF LUMINESCENCE DATA

Heating-induced changes in the intensity of luminescence, although generally in the predicted direction, are very erratic when compared with conventional indicators of thermal maturity (Figs. 4, 5 and 6). The possibility that the conventional indicators are rather inexact monitors of thermal history must be considered. In addition, the response of a given natural calcite to heating may reflect variables other than thermal history (e.g. crystal growth, deformation) . Compared with synthetic calcite the changes in CL induced by heating rocks are more complex in that both the wavelength and emission band width may change. When rocks are heated there may be chemical exchanges which do not occur in synthetic calcite.

There are no objective criteria available against which the reliability of the CAI, Ro and TAI values for the samples may be judged. They can, however, be tested for internal consistency (unfortunately suitable data extend over only a limited range of CAI values). Figs. 14 and 15 make comparisons for those samples for which two or more thermal maturation indicators are known (the data are in Table 1c). Fig. 14 shows that values of Ro for a given CAI form fairly tight groupings (range of <1 in Ro) but there is no difference in Ro values between

CAI = 1 and CAI = 1.5. The TAI shows a much wider range of values for a given CAI (range >1 unit) and again, there is no difference in TAI between CAI groups 1 and 1.5. Comparing TAI and Ro (Fig. 15) it is clear that there is a positive correlation between the two parameters, but the scatter of values at low TAI and Ro is appreciable.

The inference to be drawn from these data echo that demonstrated in figures 7 and 8 of Williams & Burden (1992): high quality correlations between measures of thermal maturity are not to be expected, especially in rocks which have been subjected only to low temperatures (<90°C) Thus, it is concluded that (in part) the scatter in relationships between the CL data and the CAI data shown in Figs. 4 to 13 reflect the significant inherent limitations of the CAI method, as well as any inadequacies in the CL technique. This is not to imply, however, that either method is valueless for these rocks - the regional trends presented by Williams & Burden (1992) show otherwise - but anomalies must be expected.

Mason (in press) found that in synthetic calcite the magnitude of I_H/I was rather variable among the different starting materials used, but there was no relationship between the intensity ratio and chemical composition. The effect of heating on intensity was attributed to the destruction of (unspecified) defects which either suppress CL emission or interfere with the transfer of energy to the activator ions. It was suggested that the variability in response may reflect differing defect densities acquired during crystal growth. This may also be a factor in natural material and may explain why sample BP-1, a Recent precipitate, showed only modest response to heating.

It is clear both in the field and in thin section that some of the rocks studied have been deformed. This is particularly true of those samples taken from beneath the Hare Bay allochthon. In the field, the deformation manifests itself in the form of conspicuously folded and extended dolomite-rich layers, which may once have been worm burrows. On a microscopic scale, the development of twin lamellae in calcite and, in one sample, the presence of quartz with undulose extinction, are indicative of deformation. If Mason's (in press) hypothesis that defects are important in controlling CL intensity is correct, then deformation might influence the CL intensity through the development of the dislocations which allow various slip mechanisms to operate (see, for example, Wenk et al., 1983). It can be anticipated that if such dislocations are important to CL then the relative timing of deformation and low-grade metamorphism may be critical, because the dislocations could be annealed out if the thermal pulse came after deformation. Thus, some of the scatter in the I_H/I values within each CAI group may reflect differences between the samples in the extent and timing of deformation.

The material studied differs from the synthetic calcite of Mason (in press) in being heterogeneous: calcite and dolomite are detectable by XRD in the majority of samples, and may be present below the detection limit (~1%) in all. A contribution to the relatively erratic behaviour of the intensity ratio could arise if, during heating, Mn and/or Fe (a known quencher of CL emission) are redistributed between calcite dolomite. It should be noted, however, that there is no direct evidence for such an effect. Indeed, Mason (in press) found no evidence (in the zoning patterns) for significant transport of Mn within heated single crystals of synthetic calcite.

A further difference between rocks and synthetic calcite lies in their respective compositions. The latter, having been grown under controlled conditions, contains elements such as Fe and Mg at concentrations <<100ppm. In contrast, preliminary electron microprobe work indicates that Mg is present at the 0.2 to 0.5 wt% level and Fe is present at up to 0.1 wt% in the natural calcites.

The wavelength of CL emission for an activator depends on the average coordination environment, which is a function of composition and mixing properties. In the present case it is the concentration of Mg and the nature of Ca-Mg mixing which are expected to exert the greatest influence on wavelength. A compositional effect on the emission band width could arise from the wider range of coordination environments possible in crystals of low purity. In addition, because calcite in the natural samples coexists with dolomite, there is the possibility of exchange of Ca and Mg between these two phases during heating. These effects are explored in detail below.

Under equilibrium conditions, the concentration of Mg in calcite coexisting with dolomite at a fixed temperature is defined by the limb of the calcite-dolomite miscibility gap. (This is almost universally referred to as a "solvus", even though the gap exists between phases of different structure) . The solvus has been located in temperature-composition space by Goldsmith & Heard (1961) and Goldsmith & Newton (1969) and is presented in Fig. 16a. Owing to experimental difficulties, the solvus limb positions are not well constrained

below 300°C, but it is expected that calcite equilibrated below this temperature will contain <1 mole% $MGCO_3$ (approximately 0.2 wt% Mg).

It is well known that biogenic carbonates are precipitated metastably as either high magnesium calcite (HMC), containing 4-30 mole% $MgCO_3$, or as aragonite (see, for example, Veizer, 1983). During diagenesis both phases transform towards (more) stable low magnesium calcite (LMC, <4 mole% $MgCO_3$). That is to say, calcite compositions initially inside the solvus should migrate towards the Ca-rich limb, along paths such as A and B in Fig. 16a. The excess Mg is released to the pore fluid and may be re-precipitated as dolomite. As with any reaction, it is to be expected that the rate of compositional change, and the final extent of re-equilibration, will be greater at high- than at low-temperature. Thus, in rocks which have been subjected to a relatively high temperature (A on Fig. 16a), calcite composition is likely to approach the solvus limb more closely than in rocks which have experienced low temperatures (B on Fig. 16a).

The wavelength of CL emission from calcite: Mn is known to increase as Mg content increases (Sommer, 1972; Marshall, 1988). Thus, qualitatively, the trend of decreasing emission wavelength with increasing CAI (Fig. 7) can be explained by the above hypothesis as arising from a greater extent of equilibration towards the solvus limb, and therefore possession of lower Mg contents, in calcite from rocks with higher CAI.

When heated in the laboratory, it is to be expected that calcite composition should re-equilibrate towards the solvus limb. Fig. 16b is a sketch of the Ca-rich solvus limb at low temperature. As noted above, the position of this limb is not well known below 300°C. For the purposes of illustration Fig. 16b was constructed from the thermodynamic data in Goldsmith & Newton (1969) using a regular solution model at 1 atmosphere pressure. In reality the solvus is asymmetric (i.e. non-regular) and there is a small pressure effect on the limb position.

Any calcite with a composition inside the solvus should reduce its Mg content during laboratory heating (by Ca/Mg exchange with pre-existing dolomite or precipitation of new dolomite). Any calcite with a composition outside the solvus should increase its Mg content. Consider a calcite such as C on Fig. 16b. Having equilibrated to the solvus limb during low-grade metamorphism, the composition lies outside the position of the solvus limb at 400°C. On heating at 400°C in the laboratory, the Mg content is too low and should increase, leading to an increase in the wavelength of CL emission after heating. Conversely, low temperature calcite (D on Fig. 16) may retain (metastably) a relatively high Mg content an lie inside the solvus. On heating in the laboratory, such a calcite should lose Mg by Ca/Mg exchange with dolomite, resulting in a decrease in the wavelength of CL emission. In this way the pattern of variation in $\Delta\lambda$ as a function of CAI (Fig. 9) can be explained.

Although the hypothesis presented above accounts qualitatively for the observations pertaining to wavelengths, and changes in wavelength induced by heating, there are some problems. Firstly, the rate of increase of emission wavelength with mg concentration is approximately 1 nm/mole% $MgCO_3$, according to Sommer (1972, fig. 2) . This requires a compositional range of 20 mole% $MgCO_3$ across the samples in order to explain the observed range in emission wavelengths (approximately 20 nm) from control material. A program of microprobe analysis of control material has just commenced and, although data are available for only five samples, the highest $MgCO_3$ content encountered is only 1.5 mole%. In addition, the magnitude of the changes in emission wavelength on heating ($\pm$20 nm, Table 1b) require rather dramatic compositional changes ($\pm$20 mole% $MgCO_3$) to take place.

These magnitudes are predicted on the basis of a shift in wavelength of 1nm per mole% $MgCO_3$ which is linear across the calcite-magnesite system (Sommer, 1972, fig. 2). It is possible that the scatter in this relationship (loc. cit.) conceals deviations from linearity resulting from non-random mixing of Ca and Mg. Such non-random mixing is to be expected because the presence of a solvus in the system calcite-dolomite shows that Ca- Mg mixing must be non-ideal. It can be argued from crystal field theory that the wavelength of emission from Mn^{2+} in calcite should be very sensitive to local coordination environment, which is a function of both the concentrations and mixing of Ca and Mg. If there is any tendency to form Ca-rich and Mg-rich clusters in the structure, it is to be expected that the rate of increase of wavelength with composition will be steeper that is suggested by Sommer's (1972) data. Nevertheless, until the suggested influence of Ca-Mg mixing is verified experimentally, the observed magnitude of the compositional effect on wavelength stands as an argument

against the proposed explanation of the wavelength versus CAI systematics.

Secondly, it was observed (Fig. 13) that the emission band generally becomes narrower on heating material with higher CAI and gets broader on heating material of low CAI. This pattern is difficult to reconcile with the hypothesis outlined above.

It would be expected that an increase in Mg content during heating would lead to an increase in emission band width because a wider range of coordination environments is possible in less pure calcite. Again, however, this argument may be simplistic in neglecting the possible influence of Ca-Mg mixing on emission band width.

REGIONAL TRENDS

From the data presented above, it may be anticipated that parameters derived from CL spectroscopy have some value in delineating regional trends in thermal maturity.

Fig. 2 shows the CAI data for the sample localities of the present work (CAI data from Williams & Burden, 1992). There is a very clear trend of decreasing CAI from north-east (Quirpon) to south-west (Port aux Port Peninsula). Contours of equal CAI would lie NNE-SSW, with values decreasing to the west. This distribution provides a standard against which the CL data can be compared.

Fig. 17 illustrates the geographical distribution of CL intensity ratios. There is a general-trend of increasing I_H/I from north-east to south-west, in conformity with the spatial distribution of CAI. The trend is seen most clearly in the mean values of I_H/I (circles on Fig. 17): the scatter of data for individual localities is considerable, as would be expected from the relationship between I_H/I and CAI shown in Fig. 4.

A geographical trend is more clearly seen in the distribution of the change in emission wavelength on heating (Fig. 18). In the north-east (Quirpon-Pistolet Bay and adjacent areas) values are predominantly in the range 1 to 19. In the Port aux Choix - Bonne Bay areas the values are in the range 0 to -12 and on the Port aux Port Peninsula and immediately adjacent areas the values lie in the range -1 to -19. The gradient in this parameter therefore lies essentially E-W and contours would essentially parallel those of CAI. As could be anticipated from the results presented in Fig. 9, the systematic geographical trend for this parameter is not so well defined as that for CAI.

Fig. 19 illustrates the geographical distribution of the change in emission band width on heating. In the north-east the values are dominantly in the range 1 to -27. In the Port aux Choix to Bonne Bay areas values of ΔFWHM are in the range -1 to 11. On the Port aux Port Peninsula and adjacent areas most values are in the range 7 to 11. Once again, if contours in this parameter were constructed they would lie essentially parallel to those for CAI.

DISCUSSION OF REGIONAL TRENDS

The data presented above essentially conform to the regional pattern of variation demonstrated by the CAI data: thermal maturity in the Cambro-ordovician carbonate sequence of Western Newfoundland increases from west to east. However, the parameters derived from the CL data do not vary with geography in so consistent a manner as do the CAI values. This could be anticipated from the quality of the correlations presented in Figs. 4, 9 and 13.

The CL method provides three parameters which have some value in measuring thermal maturity: intensity ratio (I_H/I) , change in emission wavelength ($\Delta\lambda$) and change in emission band width (ΔFWHM) . That is to say, these parameters correlate with a conventional measure of thermal maturity (CAI) and appear to define a similar

regional pattern. Their principal disadvantage is that measurement of an individual sample is insufficient to provide reliable data: the geographical trends displayed only emerge when comparatively large numbers of samples are studied. Of the three parameters, the change in emission wavelength is the most reliable.

A question which arises immediately is whether the CL data reflect local subtleties in thermal maturity which the CAI data do not, a possibility which must be entertained given that the degree of internal consistency between the CAI, TAI and Ro values is only moderate (Figs. 14 and 15). Unfortunately, from the data presently available, this question cannot be answered. As discussed above, the problem may lie either with the inherent uncertainties of the CAI method, or with the complexities of the processes which may occur in heterogeneous material when it is heated.

CONCLUSION

(1) Heating of natural limestone at 400°C induces changes in CL intensity from calcite. The changes are measured by the intensity ratio which ranges from 0.3 to 2.8, similar to the values obtained on synthetic calcite.

(2) There is a (poorly defined) negative correlation between the intensity ratio and CAI, consistent with expectations. The scatter in this relationship is attributed to the limitations of the CAI, to the possible effects of deformation and to complications arising from chemical exchange between calcite and dolomite.

(3) The wavelength (centroid) of (Mn^{2+} activated) emission from calcite lies in the range 597 to 623 nm in both heated and control (i.e. unheated) samples. The wavelength of emission from control material decreases with increasing CAI, although there is considerable scatter in the data. On heating, the wavelength (centroid) of CL emission is changed by 0 to ±20 nm, and the width of the CL emission band (FWHM) by 0 to ±27 nm.

(4) The change in emission wavelength induced by heating ($\Delta\lambda$) shows a positive correlation with CAI, whereas the change in FWHM induced by heating, (ΔFWHM) shows a negative correlation with CAI.

(5) The regional trends in intensity ratio, $\Delta\lambda$, and ΔFWHM parallel that defined by CAI. Of the three parameters derived from CL measurement, $\Delta\lambda$ and ΔFWHM offer the best prospects for practical use, although measurements on a single sample cannot be considered a reliable indicator of thermal maturity. Regional trends in the intensity ratio only become apparent when relatively large numbers of samples are available.

(6) The presence of dolomite in the samples, and the more complex chemistry of rocks compared with synthetic calcite, leads to the greater complexity in their behaviour on heating.

(7) The relationship between the wavelength of CL emission and CAI in control material can be explained qualitatively in terms of differences the extent of partial compositional equilibration towards the limb of the calcite-dolomite solvus. The relationship between $\Delta\lambda$ and CAI can be explained (qualitatively by redistribution of Ca and Mg between calcite and dolomite during laboratory heating. There are quantitative problems with these explanations which await resolution. In addition, the hypothesis does not explain the data pertaining to changes in FWHM induced by heating.

(8) The usefulness of CL as a means of (indirect) palaeotemperature estimation has been established in the present work. However, some improvements are desirable to enhance the application of the technique.

FUTURE WORK

The most important improvement will be the determination of the cause (s) of the differing response of CL intensity to heating among samples with (apparently) similar thermal history. This may allow reliable results to be obtained from measurements on a single sample. From the discussion presented above, the factors to be addressed are:

(1) characterization of control material with respect to defect density and composition;
(2) characterization of heated material with respect to these parameters;
(3) evaluation of the role of deformation in modifying CL;
(4) calibration of the CL measurements against a reliable temperature scale.

From a more academic standpoint, measurement of the effects of Ca-Mg mixing properties on CL emission wavelength and band width is highly desirable.

This work will require a refinement of the techniques used to date. The greatest change will be the study of single crystal material, or slabbed and polished rock sections. This will allow CL and chemical measurements to be made at the same locations (on a scale of 50 to 100 μm) before and after heating. One advantage of this "microscopic" approach is that it should allow comparisons to be made between different compositional and textural areas in a single sample. The facilities for this kind of work are available in-house.

Calibration of natural material against reliable temperature scales will be more difficult. The two most promising techniques are fluid inclusion studies and oxygen isotope thermometry. Both techniques are available within CERR, but success depends critically on the provision of suitable samples.

The role of deformation could be addressed experimentally in work on single crystals. At present the level of experimental sophistication required is unclear, however, simple pilot studies should be simple and inexpensive to initiate.

REFERENCES

Goldsmith, J.R. & Heard, H.C. (1961) Subsolidus phase relations in the system $CaCO_3$ - $MgCO_3$. Journal of Geology, 69, 45-74.

Goldsmith, J.R. & Newton, R.C. (1969) P-T-X relations in the system $CaCO_3$ - $MgCO_3$, at high temperatures and pressures. American Journal of Science, 267-A, 160-190.

Machel, H.G., Mason, R.A., Mariano, A.N. & Mucci, A. (1991) Causes and emission of luminescence in calcite and dolomite. In: Luminescence Microscopy and Spectroscopy: Qualitative and Quantitative Applications. C.E. Barker & O.C. Kopp, editors. SEPM Short Course Notes 25, 9-25.

Marshall, D.J. (1988) Cathodoluminescence of Geological Materials. Unwin Hyman, Boston.

Mason, R.A. (1992) Evaluation of Cathodoluminescence as an Indicator of Thermal Maturity in Limestones. CERR Report to
Mobil Oil Canada.

Mason, R.A. & Mariano, A.N. (1990) Cathodoluminescence activation in manganese-bearing and rare earth-bearing synthetic calcites. Chemical Geology, 88, 191-206.

Mason, R.A. (in press) Effects of heating and prolonged electron bombardment on cathodoluminescence emission in synthetic calcite. Accepted for publication in Chemical Geology, Dec. 1992.

Sommer, S.E. (1972) Cathodoluminescence of carbonates, 1. Characterization of cathodoluminescence from carbonate solid solutions. Chemical Geology, 9, 257-273

Veizer, J. (1983) Trace elements and isotopes in sedimentary carbonates. In: Carbonates: Mineralogy and Chemistry. R.J. Reeder, editor. Mineralogical Society of America, Reviews in Mineralogy 11, 265-299.

Wenk, H.R., Barber, D.J. & Reeder, R J. (1983) Microstructures in carbonates. In: Carbonates: Mineralogy and Chemistry. R.J. Reeder, editor. Mineralogical Society of America, Reviews in Mineralogy 11, 301-367.

Williams, S.H. & Burden, E.T. (1992) Thermal Maturity of Potential Paleozoic Source Rocks in Western Newfoundland. CERR Report to Mobil oil Canada.

[Home] [Top]

Table1a. Sample numbers, descriptions & sources of thermal maturity data.		
Sample Number	**Description & Stratigraphic Age**	**Source of thermal maturity data**
F88016d	Finely recrystallised dark limestone with coarse dolomite. Llanvirn.	CAI from W & B Fig.1.
F88015	Fine dark limestone with diagenetic structure & stylolites. Llanvirn.	CAI from W & B Fig.1.
F88018b	Vein calcite from deformed marble. Age uncertain.	Discordant vein, local CAI, TAI & Ro% data not valid
Mob4	W & B (1992) field designations: 5/6/91 8b Llanvirn.	CAI, TAI & Ro% from W & B Fig.10. TAI & Ro% values are averages for this locality.
F88022	Grey limestone with pale buff dolomite defining rubbly texture. Arenig.	CAI from W & B Fig. 13.
Mob6	W & B (1992) field designations: 5/6/91 8a Llanvirn.	CAI, TAI & Ro% from W & B Fig. 10. TAI & Ro% values are averages for this locality.
F88007	Fine grained limestone with diagenetic structures. Llanvirn.	CAI from W & B Fig. 1.
F88017b	Recrystallised limestone with deformed dolomitised burrows.Llanvirn.	CAI from W & B Fig. 1.
F88011	Recrystallised limestone with calcite patches & veins. Llanvirn.	CAI estimated from W & B Fig. 1.
BP-1	Recent calcite precipitate	
F88008	Fine grained dark laminated limestone with diagenetic structures. Llanvirn.	CAI estimated from W & B Fig.1.
Mob1	W & B (1992) field designation: 6/6/91 3a Llanvirn.	CAI, TAI & Ro% from W & B Fig. 10.
F88018a	Deformed grey marble. Llanvirn.	CAI estimated from W & B Fig. 1.
F88029a	Fine dark grey limestone. L. Cambrian.	CAI, TAI & Ro% from W & B Fig. 5.
F88010	Finely laminated limestone with calcite veins (2-3 mm). Llanvirn.	CAI estimated from W & B Fig.1 .
Mob2	W & B (1992) field designation: 4/6/91 3. Llanvirn.	CAI, TAI & Ro% from W & B Fig. 13.
Mob10	W & B (1992) field designation: 5/6/91 7. Tremadoc.	CAI estimated from W & B Fig. 10, TAI estimated from W & B app. 1.
F88013	Fine grained dark limestone with diagenetic structures. Llanvirn.	CAI from W & B Fig.1.
F88028	Fine grained grey to pale buff laminated limestone. L. Cambrian.	CAI from W & B Fig.5. TAI & Ro% averages this locality, W & B Fig.5.
Mob3	W & B (1992) field designation: SPN43A. U. Tremadoc.	CAI (estimated) TAI & Ro% from W & B Fig. 5.
F8809	Fine grained dark limestone. Arenig.	CAI from W & B Fig. 1.
Mob5	W & B (1992) field designation: W. et al. '87. L. Arenig.	CAI, TAI & Ro% from W & B Fig. 13.

F88016b	White/grey facies of F88016 group. Llanvirn.	CAI from W & B Fig.1.
F88030	Fine grained limestone with diagenetic structures. Arenig (?).	CAI estimated from W & B Fig. 10.
F88020	Fine grained dark limestone. Llanvirn.	CAI from W & B Fig. 13.
F88019	Fine grey limestone with diagenetic structures. Llanvirn.	CAI from W & B Fig. 13.
Mob11	W & B (1992) field designation: 5/6/91 3 (b). L. Cambrian.	CAI & TAI estimated from W & B Fig. 5.
F88001	Coarse grey limestone with diagenetic structures. L. Arenig.	CAI, TAI & Ro% from this locality, W & B Fig. 13.
F88012	Dark fissile limestone with diagenetic structures. Llanvirn.	CAI from W & B Fig. 1.
Mob7	W & B (1992) field designation: 5/6/91 5. U. Cambrian.	CAI (estimated) & TAI from W & B Fig. 10.
Mob9	W & B (1992) field designation: 26/6/91 3 Llanvirn.	CAI from W & B Fig. 10. TAI & Ro% mean of samples this loc. W & B App. 1.
F88031	Fine to coarse limestone. Arenig.	CAI from W & B Fig. 10.

[Home] [Back]

Table 1b. Cathodoluminescence results.

Sample Number	Intensity ratio		Centroid			FWHM		
	I_H/I	+	Control	Heated	Change	Control	Heated	Change
F88016d	0.34	0.02	601	620	19	82	55	-27
F88015	0.83	0.02	604	614	10	86	79	-7
F88018b	0.83	0.01	611	612	-1	77	75	-2
Mob4	0.89	0.01	618	602	-16	82	92	10
F88022	0.90	0.01	617	617	0	82	85	3
Mob6	0.91	0.02	614	601	-13	78	89	11
F88007	1.04	0.02	620	622	2	76	69	-7
F88017b	1.12	0.02	611	610	-1	73	73	0
F88011	1.14	0.01	610	612	1	78	78	1
BP-1	1.15	0.04	611	613	2	75	75	0
F88008	1.16	0.02	600	611	11	93	88	-6
Mob1	1.18	0.04	629	622	-6	88	92	3
F88018a	1.20	0.03	611	614	3	80	80	0
F88029a	1.20	0.02	620	620	0	79	80	1
F88010	1.21	0.02	605	612	7	89	82	-8
Mob2	1.22	0.02	618	615	-3	81	85	5
Mob10	1.24	0.03	616	597	-19	83	93	10
F88013	1.25	0.02	616	617	1	71	75	4
F88028	1.28	0.03	617	616	-1	79	78	-1
Mob3	1.29	0.01	617	601	-16	78	90	12
F88009	1.30	0.04	618	613	-5	77	81	3
Mob5	1.34	0.01	619	619	0	77	79	2
F88016b	1.38	0.05	599	603	4	84	84	0
F88030	1.40	0.02	613	599	-14	76	84	8
F88020	1.40	0.02	617	608	-9	83	87	5
F88019	1.49	0.03	617	611	-6	83	86	4
Mob11	1.51	0.02	619	611	-8	79	86	8
F88001	1.54	0.04	618	606	-12	73	84	11
F88012	1.54	0.04	616	613	-3	79	80	1
Mob7	1.94	0.05	621	619	-2	78	85	7
Mob9	2.17	0.04	623	622	-1	77	83	7
F88031	2.77	0.06	621	620	-1	80	80	0

[Home] [Back]

Table 1c. Thermal maturation indicators & calcite/dolomite ratio.

Sample Number	TMI			C/D
	CAI	Ro	TAI	
F88016d	5			21
F88015	5			35
F88018b				n.d.
Mob4	1	0.62	2.1	
F88022	2			4
Mob6	1	0.62	2.1	
F88007	3.5			
F88017b	5			38
F88011	5			n.d.
BP-1				
F88008	3.5			5
Mob1	1	0.67	1.49	
F88018a	5			35
F88029a	1.5	0.56	1.44	
F88010	3.5			89
Mob2	2	1.77	3.8	
Mob10	1		2.33	
F88013	3.5			14
F88028	1.5	0.6	1.66	n.d.
Mob3	1.5	0.53	2.29	
F88009	3.5			43
Mob5	2	1.11	2.95	
F88016b	5			377
F88030	1			26
F88020	2			11
F88019	2			19
Mob11	2		4	
F88001	2	1.11	2.95	9

F88012	5			17
Mob7	1		2.33	
Mob9	1	0.73	1.18	
F88031	1			3

Notes

I_H/I = CL intensity of heated material/CL intensity of control material
FWHM = Full-width at half-maximum height
TMI = Thermal maturity indicator:
CAI = Conodont alteration index
TAI = Thermal alteration index
Ro = Vitrinite reflectance
(Data from Williams & Burden, 1992)
C/D = Calcite/Dolomite ratio, XRD estimate (n.d. = dolomite not detected).
Blank cell indicates parameter not determined.

[Home] [Back]

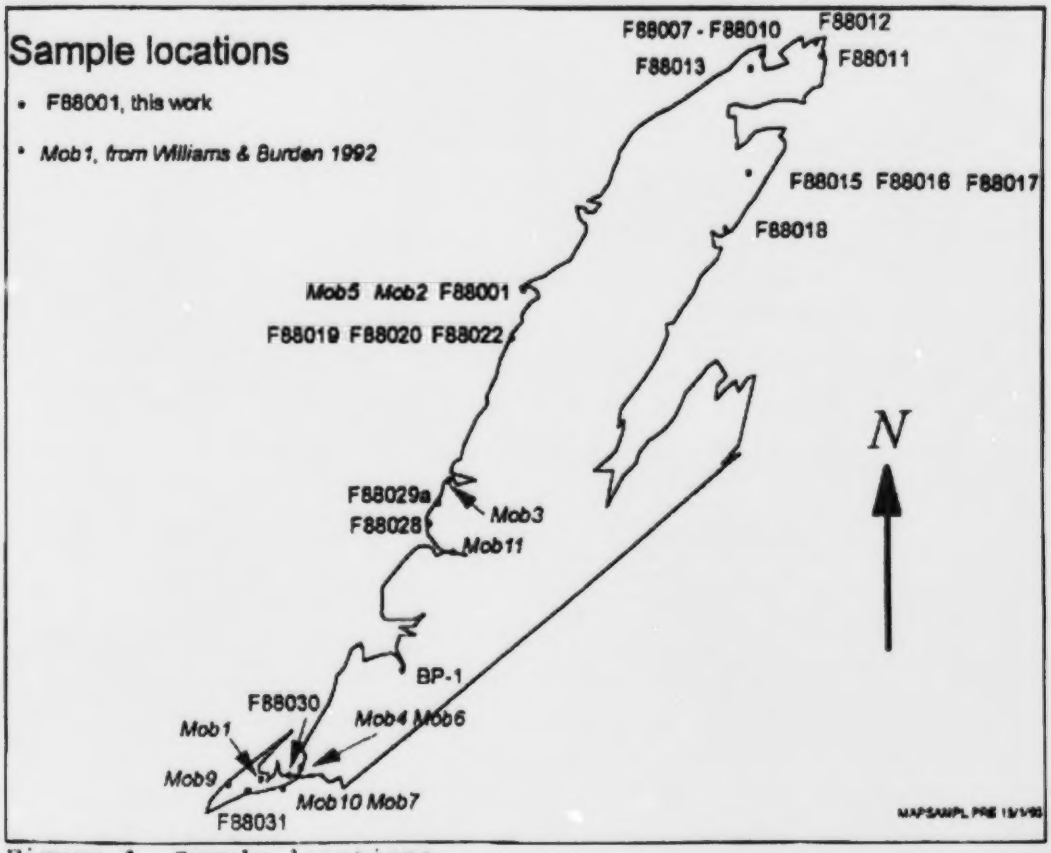

Figure 1. Sample locations.

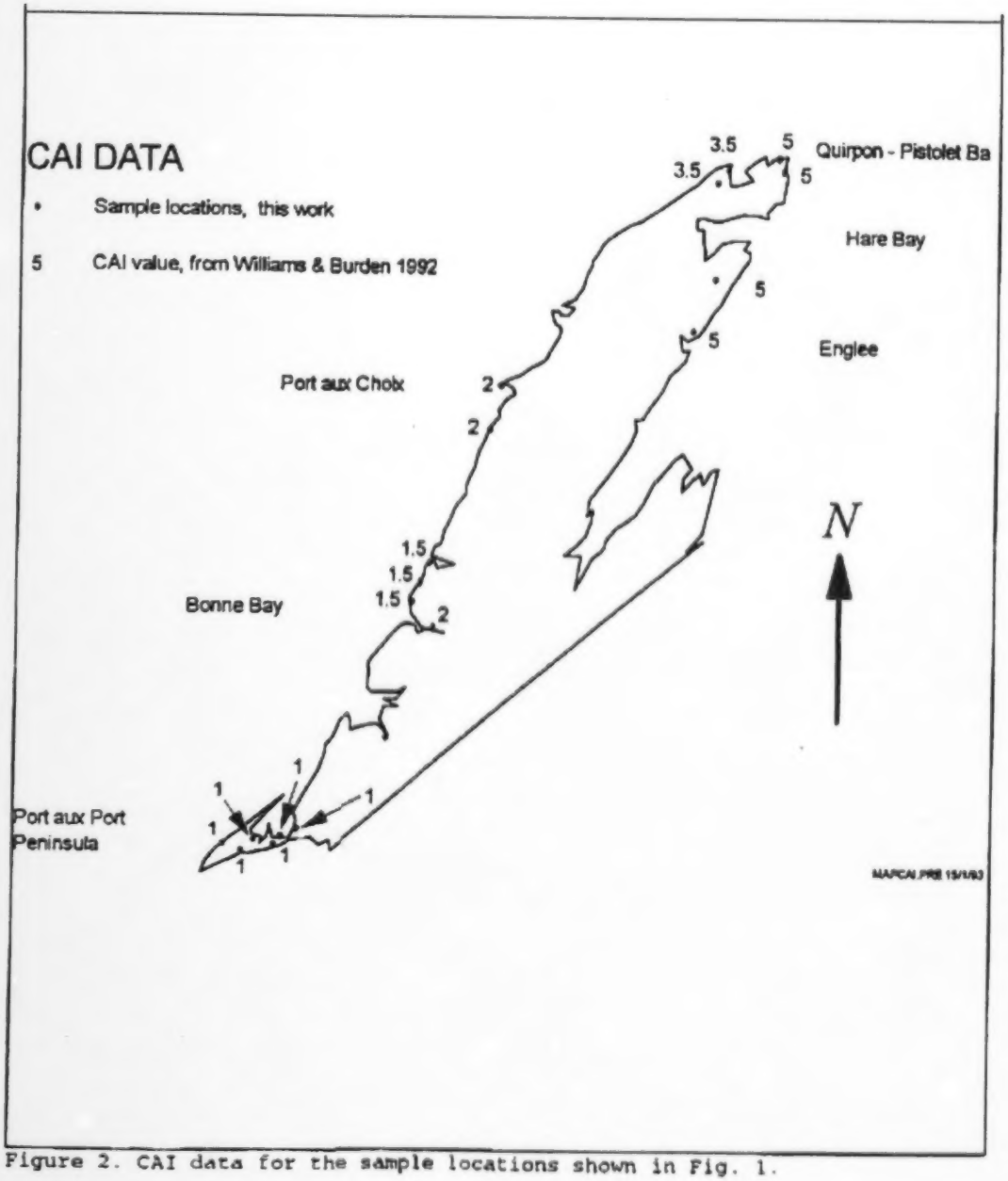

Figure 2. CAI data for the sample locations shown in Fig. 1.

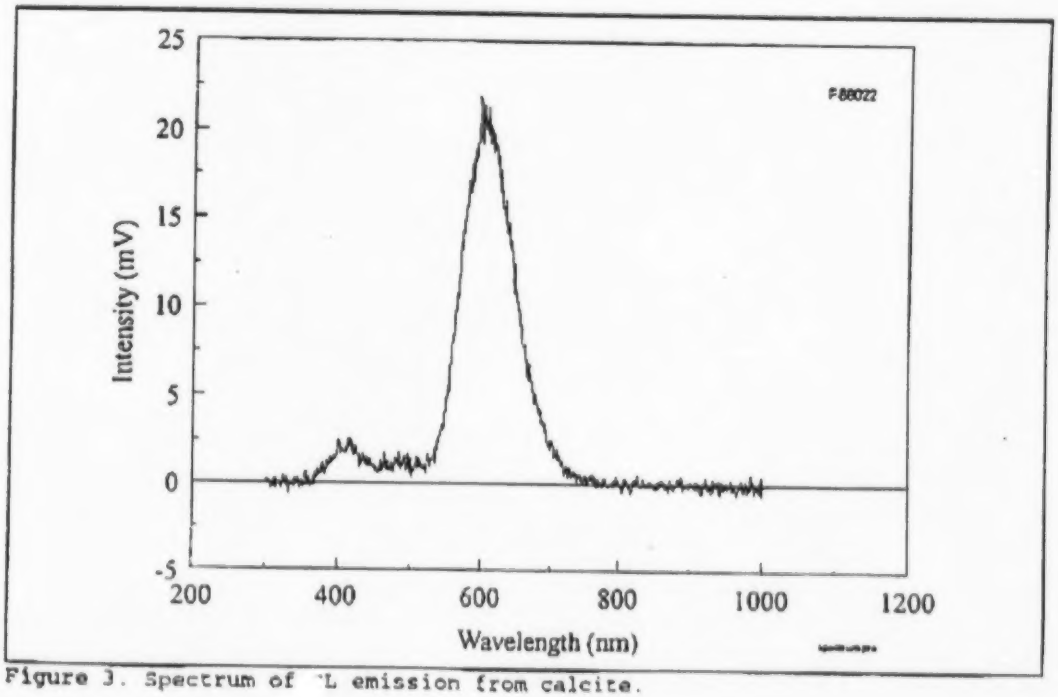

Figure 3. Spectrum of TL emission from calcite.

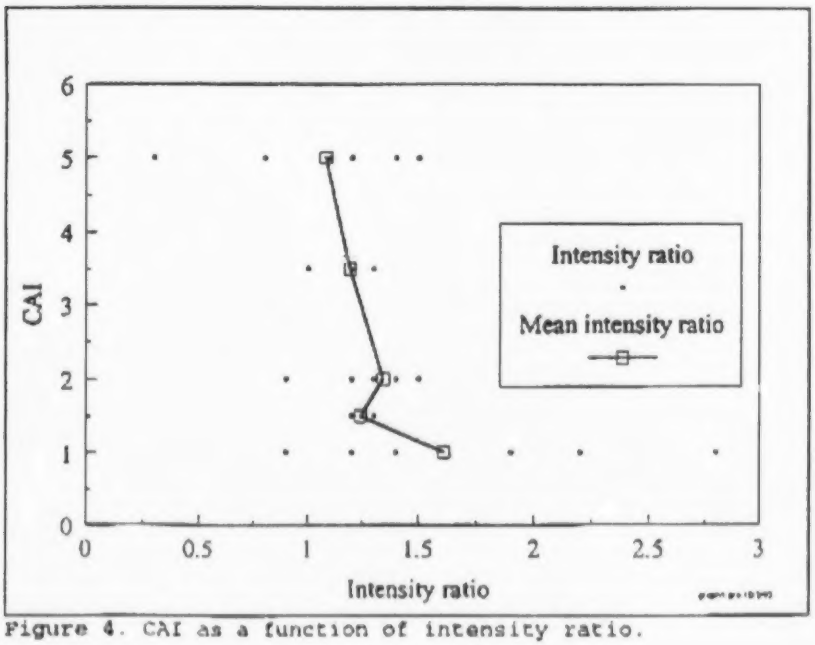

Figure 4. CAI as a function of intensity ratio.

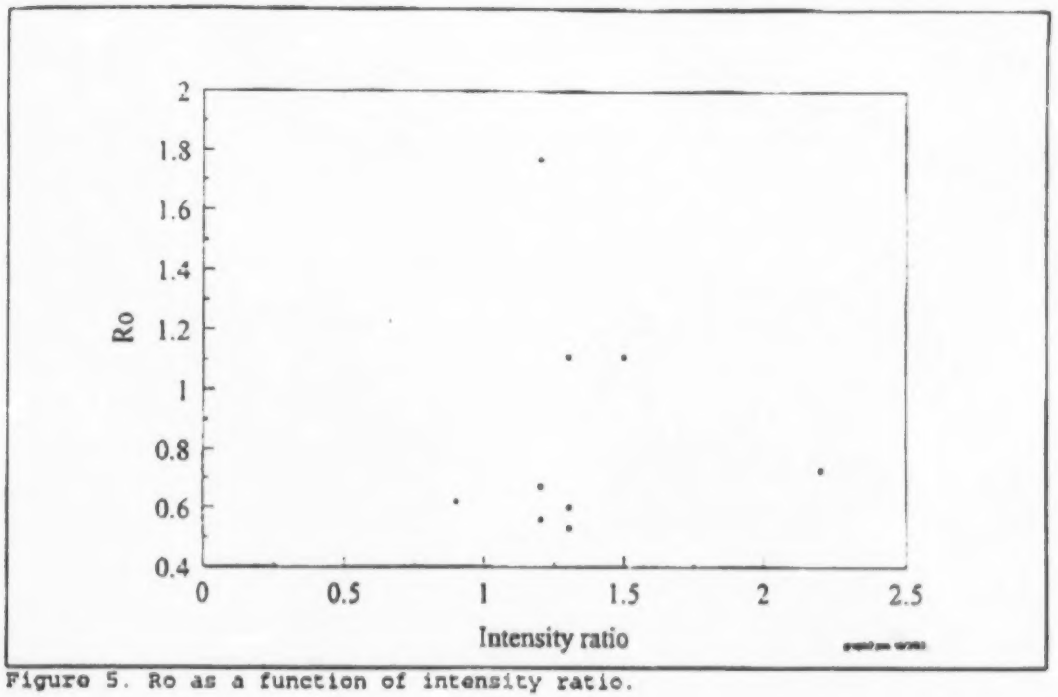

Figure 5. Ro as a function of intensity ratio.

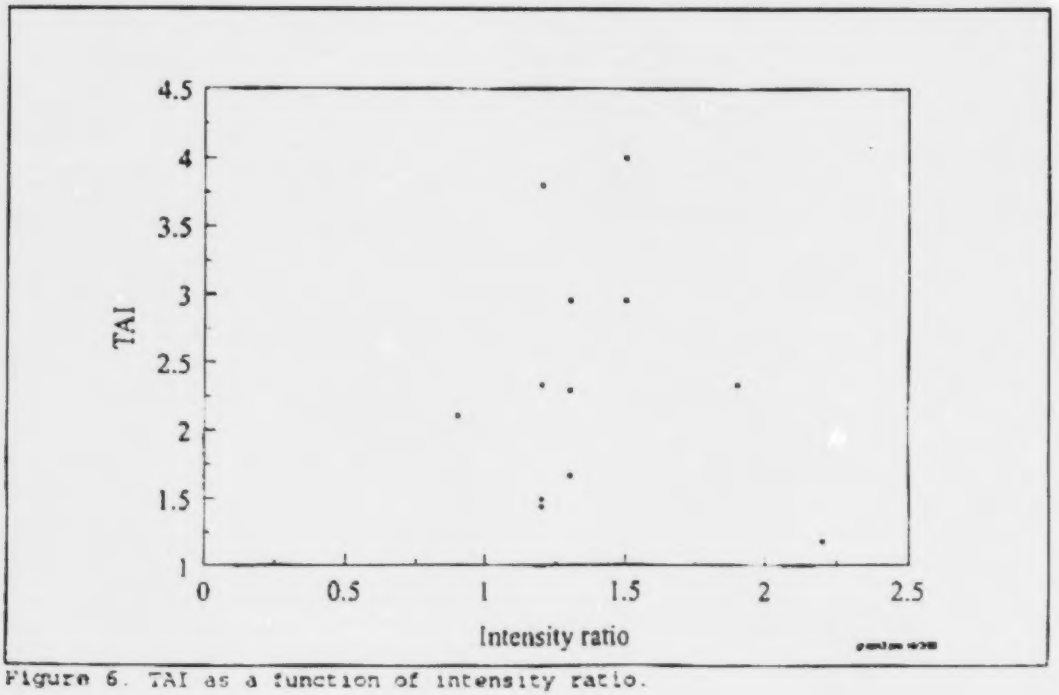

Figure 6. TAI as a function of intensity ratio.

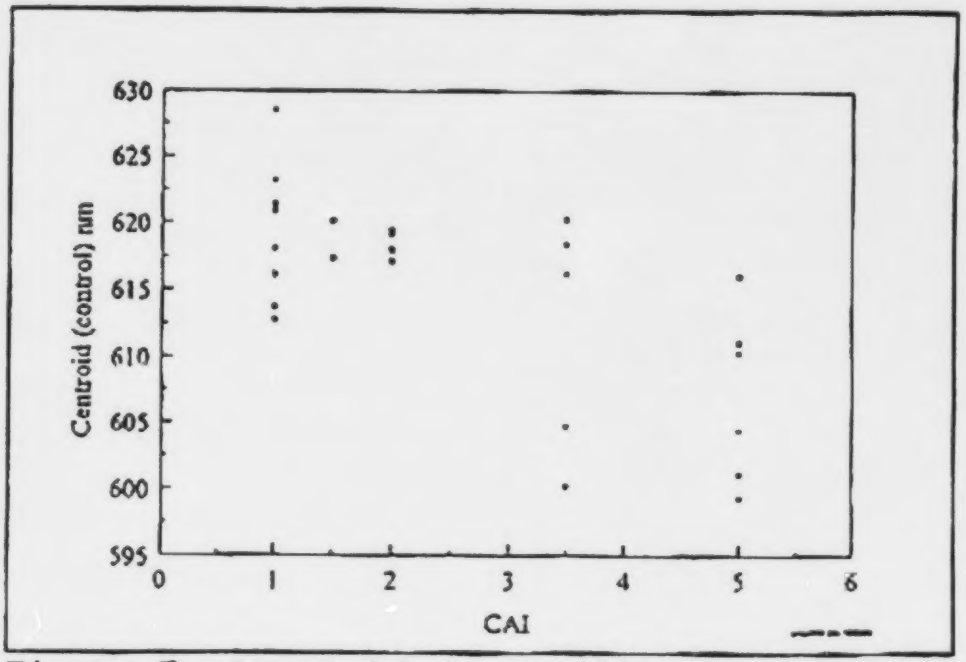

Figure 7. Centroid (control) as a function of CAI.

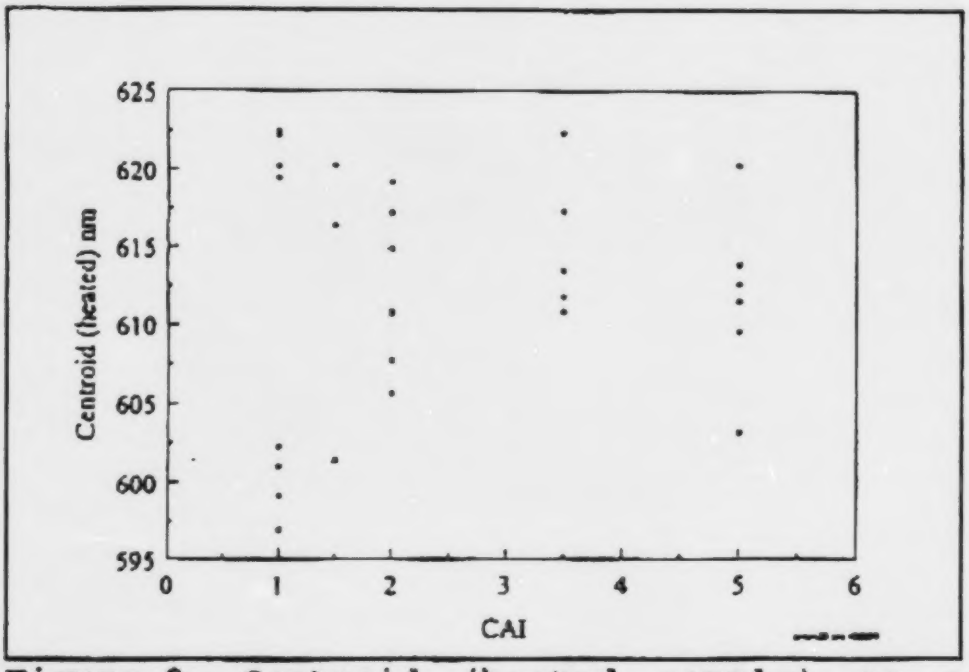

Figure 8. Centroid (heated sample) as a function of CAI.

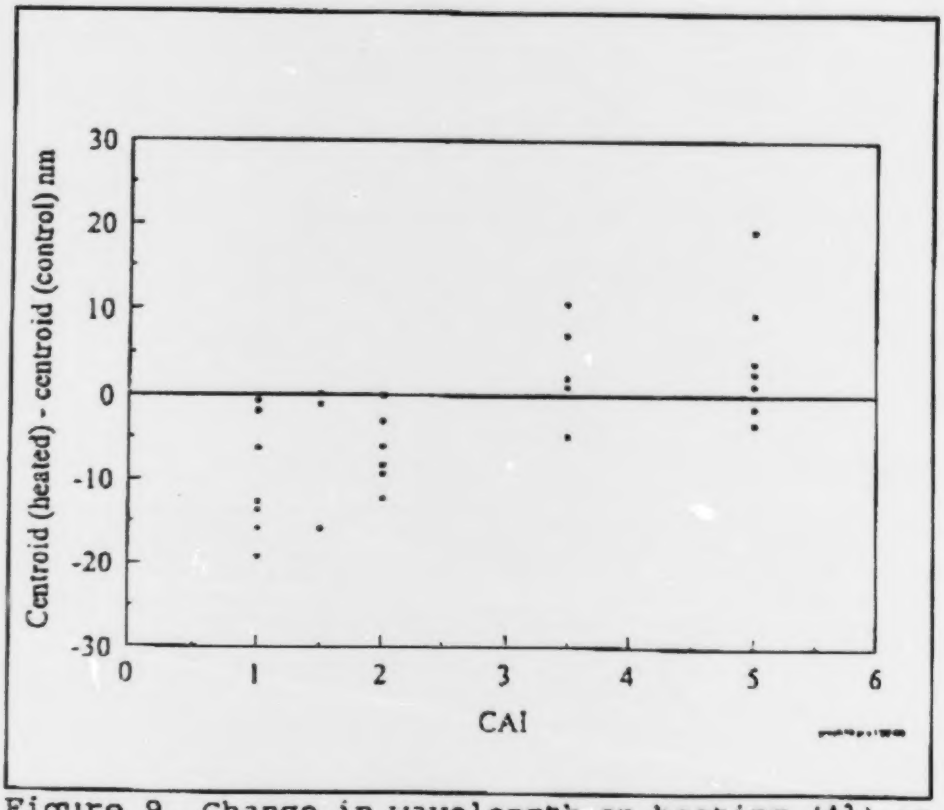

Figure 9. Change in wavelength on heating ($\Delta\lambda$) as a function of CAI.

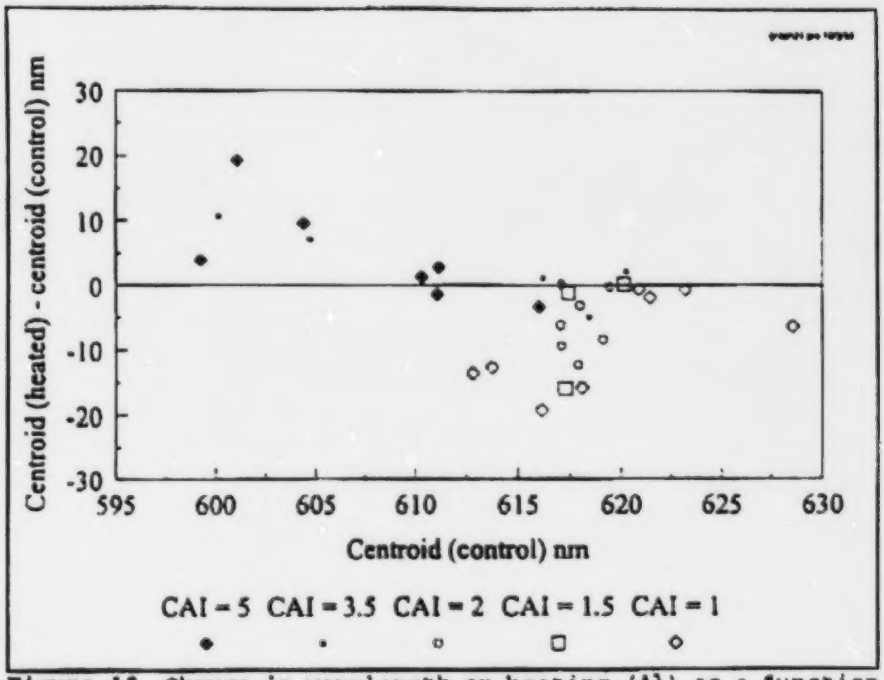

Figure 10. Change in wavelength on heating ($\Delta\lambda$) as a function of emission wavelength of control material.

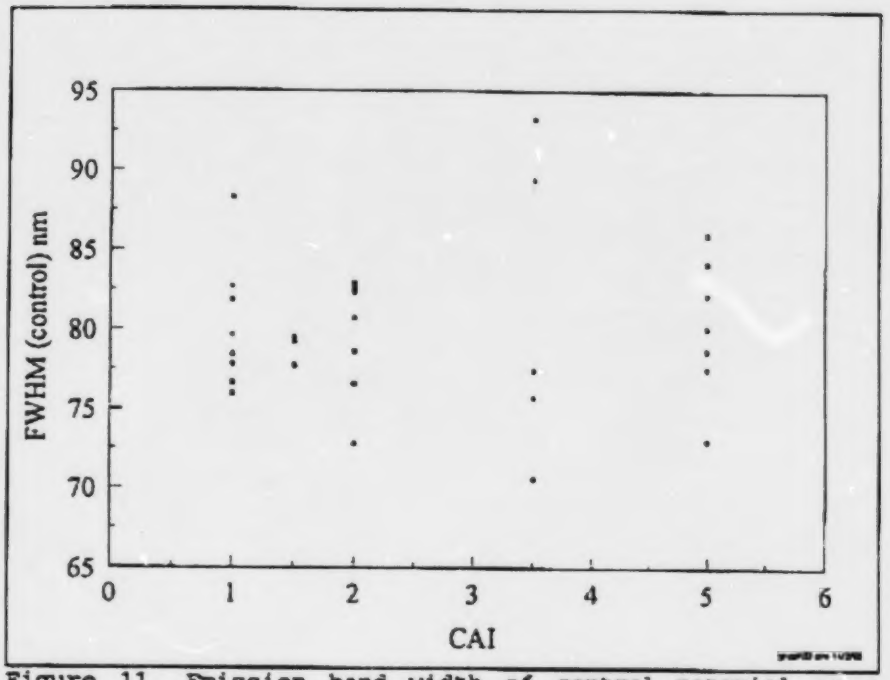

Figure 11. Emission band width of control material as a function of CAI.

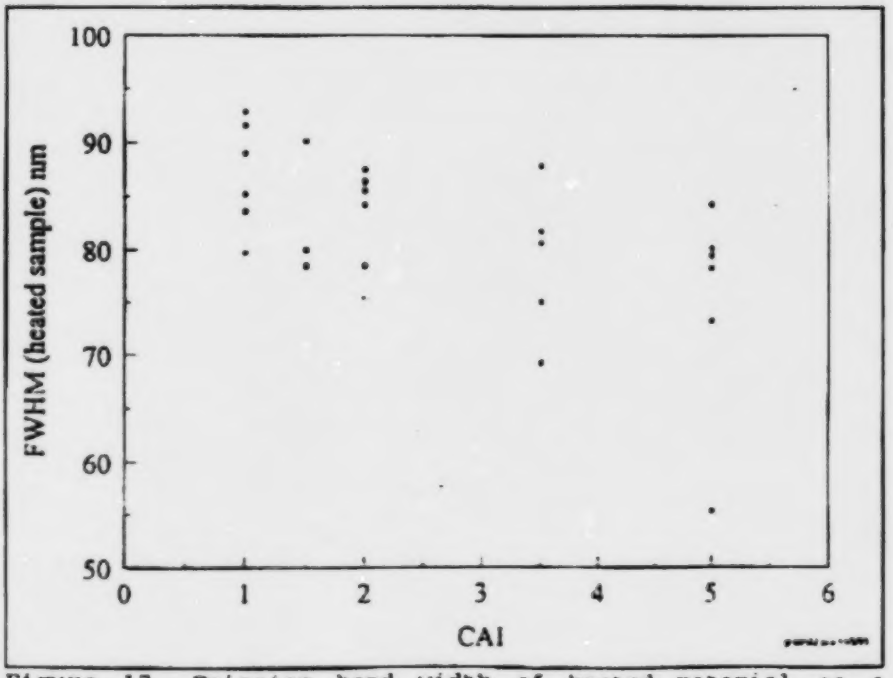

Figure 12. Emission band width of heated material as a function of CAI.

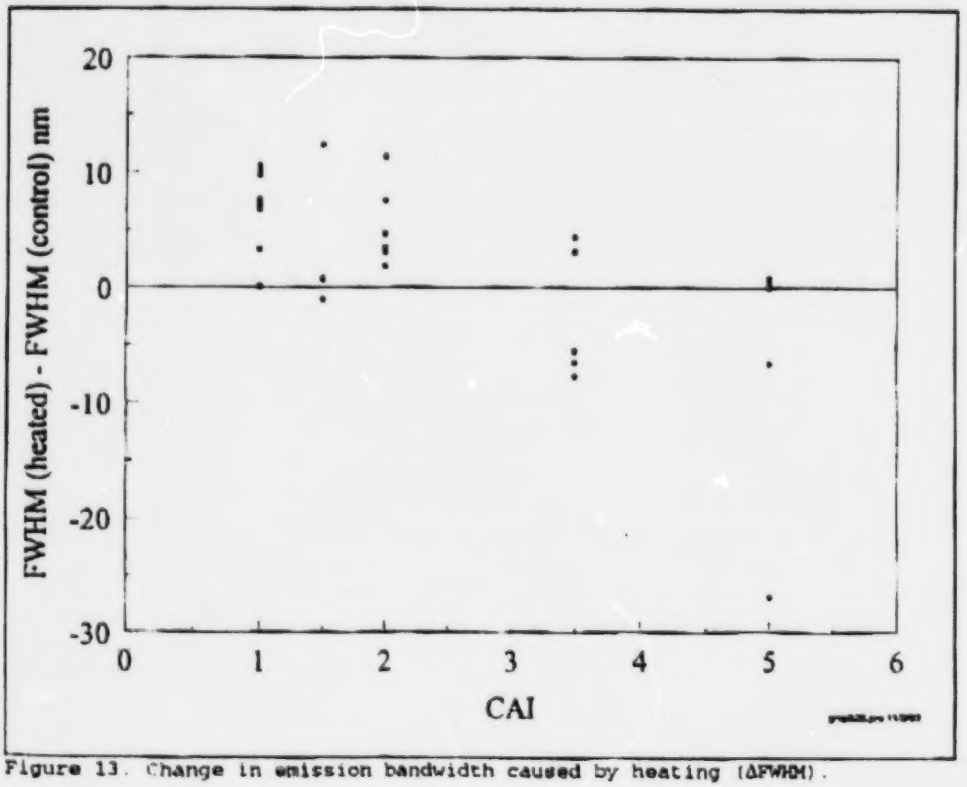

Figure 13. Change in emission bandwidth caused by heating (ΔFWHM).

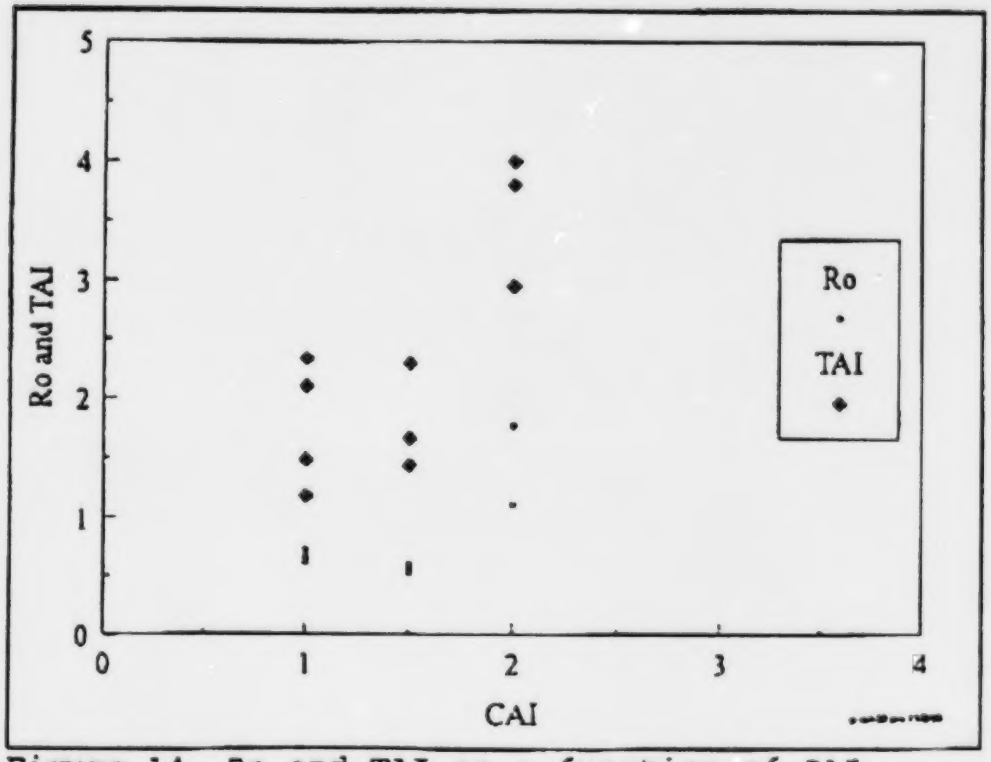

Figure 14. Ro and TAI as a function of CAI.

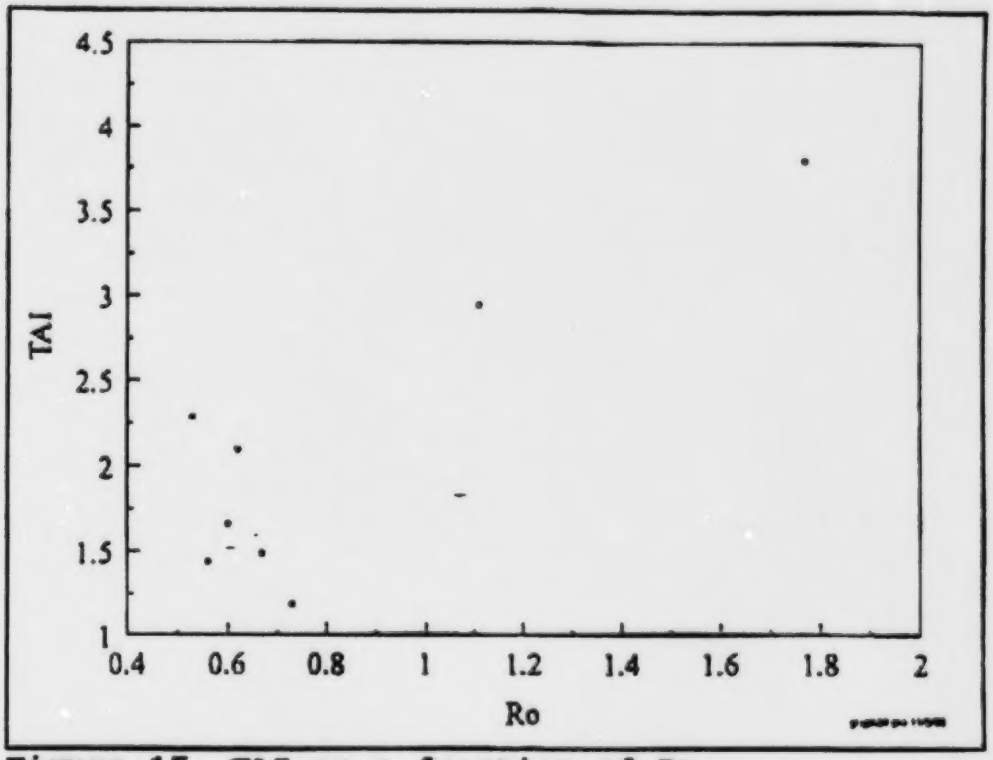

Figure 15. TAI as a function of Ro.

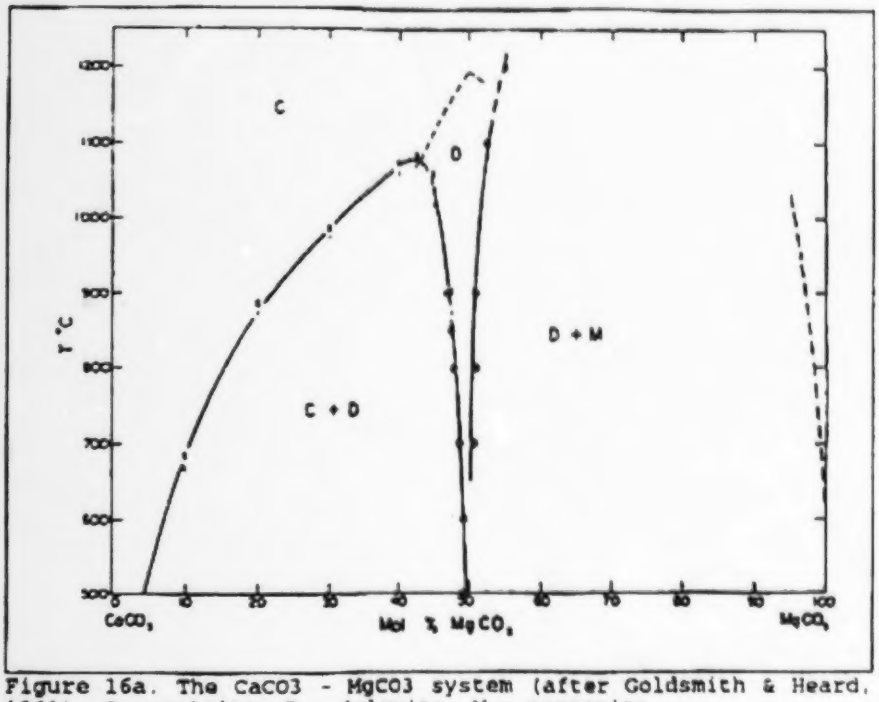

Figure 16a. The CaCO3 - MgCO3 system (after Goldsmith & Heard, 1961). C = calcite, D = dolomite, M = magnesite.

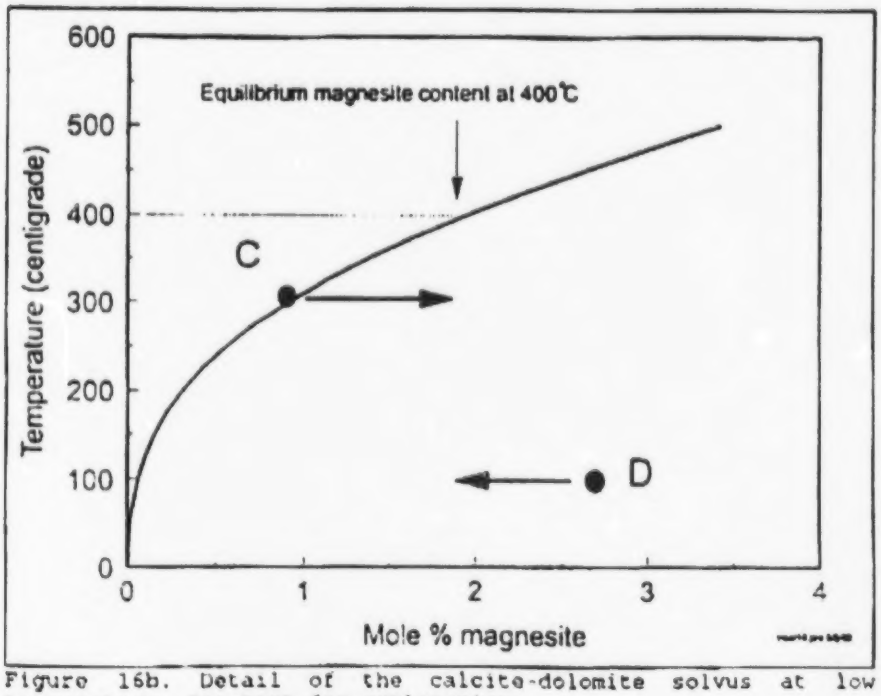

Figure 16b. Detail of the calcite-dolomite solvus at low temperature. See text for explanation.

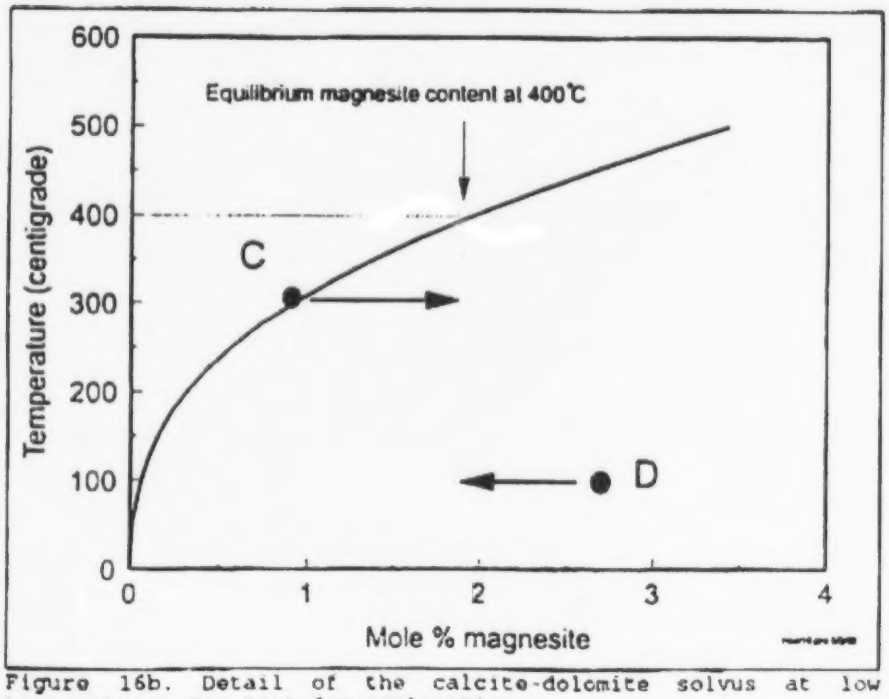

Figure 16b. Detail of the calcite-dolomite solvus at low temperature. See text for explanation.

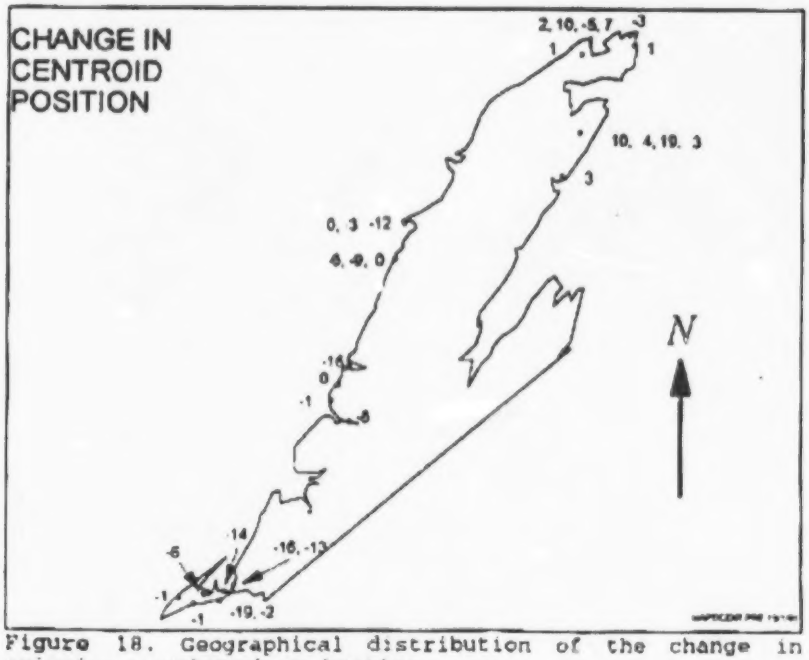

Figure 18. Geographical distribution of the change in emission wavelength on heating.

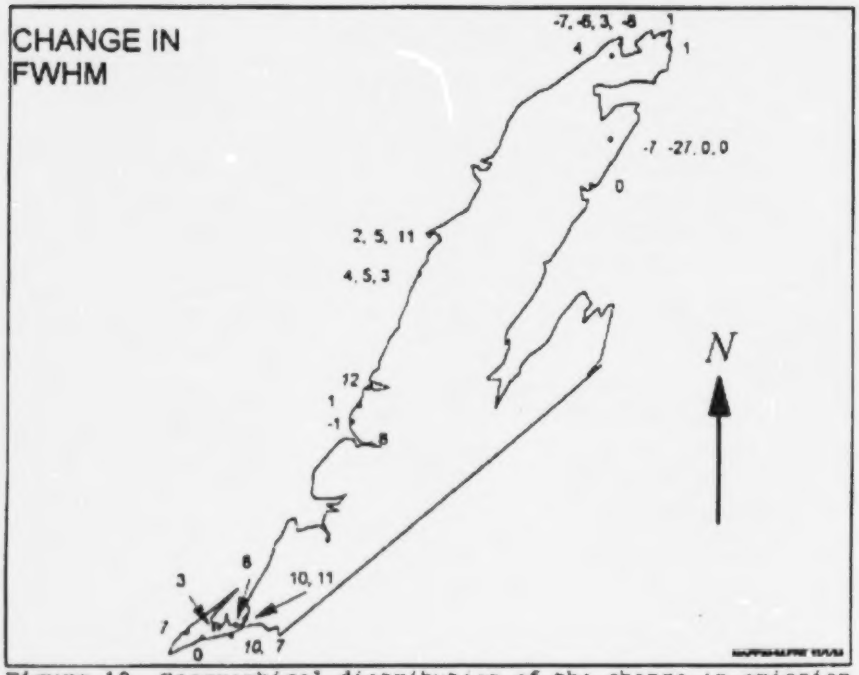

Figure 19. Geographical distribution of the change in emission band width on heating.